

www.acsabm.org Article

Passive Wireless Porous Biopolymer Sensors for At-Home Monitoring of Oil and Fatty Acid Nutrition

Kazi Khurshidi Haque Dia, Alberto Ranier Escobar, Huiting Qin, Fan Ye, Abel Jimenez, Md Abeed Hasan, Amirhossein Hajiaghajani, Manik Dautta, Lei Li, and Peter Tseng*



Cite This: ACS Appl. Bio Mater. 2024, 7, 5452-5460



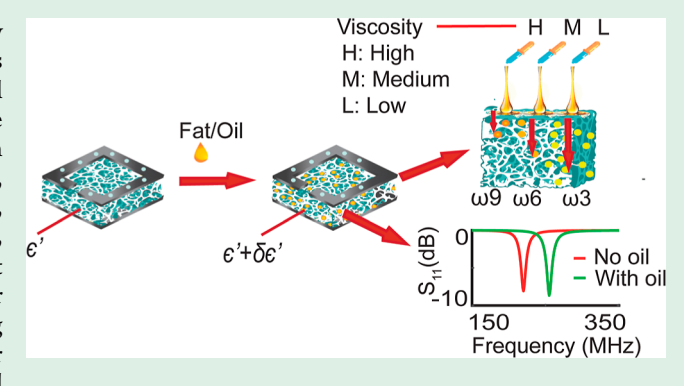
ACCESS I

III Metrics & More

Article Recommendations

sı Supporting Information

ABSTRACT: Dietary oils—rich in omega-3, -6, and -9 fatty acids—exhibit critical impacts on health parameters such as cardiovascular function, bodily inflammation, and neurological development. There has emerged a need for low-cost, accessible method to assess dietary oil consumption and its health implications. Existing methods typically require specialized, complex equipment and extensive sample preparation steps, rendering them unsuitable for home use. Addressing this gap, herein, we study passive wireless, biocompatible biosensors that can be used to monitor dietary oils directly from foods either prepared or cooked in oil. This design uses broad-coupled split ring resonators interceded with porous silk fibroin biopolymer (requiring only food-safe materials, such as aluminum foil and



biopolymer). These porous biopolymer films absorb oils at rates proportional to their viscosity/fatty acid composition and whose response can be measured wirelessly without any microelectronic components touching food. The engineering and mechanism of such sensors are explored, alongside their ability to measure the oil presence and fatty acid content directly from foods. Its simplicity, portability, and inexpensiveness are ideal for emerging needs in precision nutrition—such sensors may empower individuals to make informed dietary decisions based on direct-from-food measurements.

KEYWORDS: wireless sensors, biosensors, wearable devices, RF sensors, fat sensing, nutrient sensors, precision nutrition

1. INTRODUCTION

Recently, there has been an increasing focus on the broad impacts of dietary fat and oil consumption on human health.¹⁻⁴ Oils and fats are complex substances primarily composed of triglycerides. Triglycerides are esters formed from glycerol and fatty acids, where the fatty acids themselves can be characterized by their varying levels of saturation with hydrogen atoms. 5-8 This level of saturation is a key factor that determines the effect on health. These exhibit degrees of saturation related to the number of hydrogen atoms attached to the carbon chains of fatty acids. Saturated fatty acids have no double bonds between carbon atoms, whereas unsaturated fatty acids contain one or more double bonds. 9-11 Variation in saturation levels further leads to the formation of different types of fatty acids, notably, omega-3, omega-6, and omega-9, that exhibit increasing degrees of saturation. 12-14 While these fatty acids are essential for numerous bodily functions, they present a nuanced spectrum of health effects. 1-17 For instance, unsaturated fatty acid consumption has historically been associated with beneficial health outcomes, such as improved heart health and reduced inflammation. Conversely, saturated fats are often linked to adverse cardiac health consequences, including increases in risk of heart disease. 15-17 Omega-3 fatty

acids, prevalent in fish, chia seeds, and walnuts, have been studied for their cardiovascular protective qualities, potential mitigation of heart disease risk, and their pivotal role in brain health and cognitive function. ^{18,19} Deficiencies in omega-3 can exacerbate chronic inflammatory conditions such as rheumatoid arthritis and compromise immune responses, while an imbalance of consumption favoring omega-6—abundant in vegetable oils and processed foods—over omega-3 has been associated with metabolic disorders, including obesity and diabetes. Maintaining an optimal omega-3 to omega-6 ratio is considered important for metabolic health and inflammation control. ^{12–17} Furthermore, omega-9 fatty acids, although not essential, have been studied for their potential benefits to anti-inflammatory and anticancer effects in health. ²⁰

Dietary oil analysis typically occurs with advanced techniques such as Fourier transform infrared (FTIR)

Received: May 2, 2024 Revised: July 7, 2024 Accepted: July 9, 2024 Published: July 20, 2024





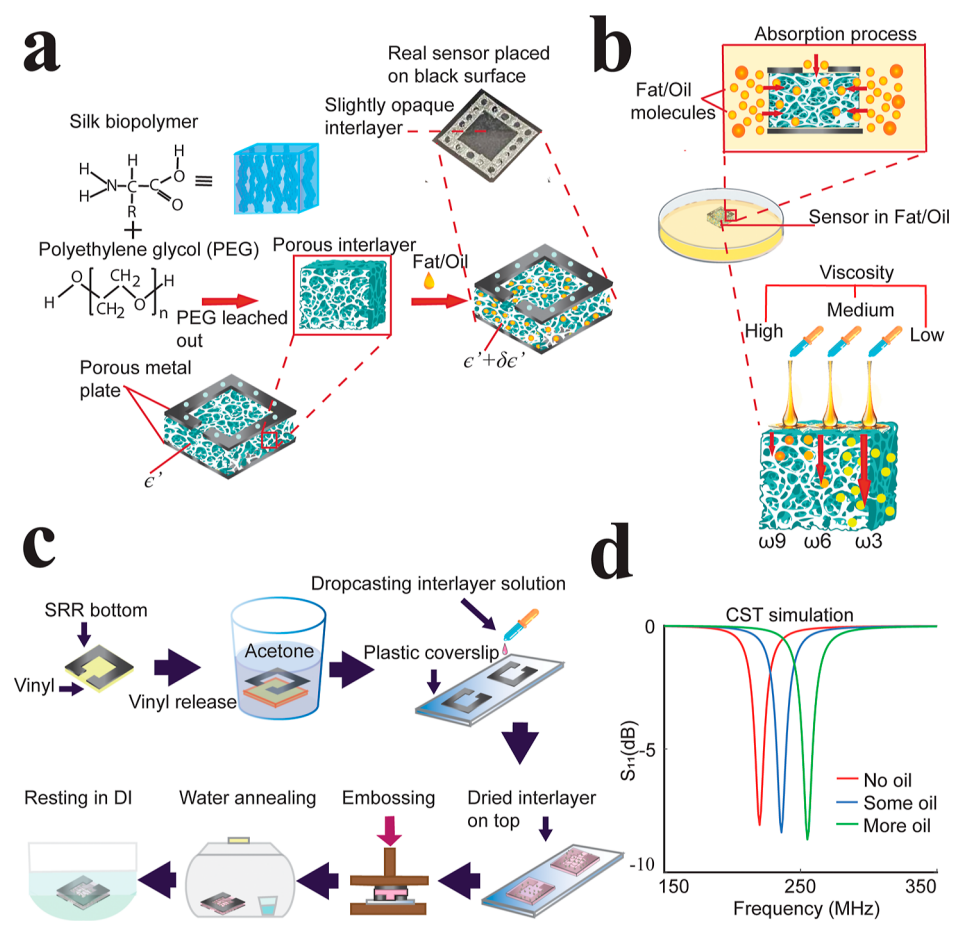


Figure 1. (a) Process for creating porous silk biopolymer via leaching of polyethylene glycol (PEG) from silk-PEG films. (b) Illustration of oil/fat absorption into the porous biopolymer as related to oil/fats viscosities. (c) Step-by-step fabrication process for the biosensor. (d) S_{11} parameter changes with oil absorption into the porous silk interlayer of the BC-SRR sensor using CST simulation.

spectroscopy, ^{21–26} gas chromatography-flame-ionization detection (GC-FID), ^{27–30} and inductively coupled plasma-mass spectrometry (ICP-MS). ^{31–35} While these techniques can typically obtain detailed information on oil fatty acid molecular composition, these each require specialized instrumentation, multiple levels of sample preparation, and specialized operational mechanisms. They thus do not meet the practical needs of at-home measurement for precision nutrition. There is a need for accessible approaches that can approximate and evaluate the composition and health implications of dietary oils directly from food. The development of such user-friendly technologies is imperative to democratize nutrition measurement, enabling individuals to make informed dietary decisions based on real-time nutritive data.

Building upon our recent advancements in biocompatible biosensors, we further study a novel approach to the at-home monitoring of oil and fatty acid consumption. At the core of our sensor is a broad-coupled split ring resonator, a passive construct composed exclusively of food-safe metal foil (herein, aluminum) and polymer. This design acts as a near-field antenna, enabling the passive, wireless monitoring of local environments. These sensors are flexible, low-cost, and are compatible with emerging wireless readout schemes. The bio amplification occurs through an interceding porous silk biopolymer, which permanently absorbs dietary oils from the environment. As these oils infiltrate the biopolymer, they induce changes in the sensor's capacitance that can be

measured wirelessly. These sensors are designed to continuously monitor increases in oil concentration; however, they operate as a one-way measurement device. Once the sensor absorbs the oil, it undergoes a permanent change in its dielectric properties, which cannot be reset to the baseline after detection. Thus, these sensors exhibit a defined lifetime related to the exposure time to oil. Our work represents a significant advancement over our previous studies,³⁹ which created similar biopolymer-based sensors for measuring sugar, salt, and oil content from liquids. Porous biopolymer-based sensors were proposed and preliminarily studied for their ability to absorb oil/fat. Here, we perform more extensive characterization and optimization of these oil-measuring sensors. We study how these sensors may potentially be used to characterize the health/nutrititive implications of dietary oils as they appear capable of discriminating omega-3, -6, and -9 fatty acid content of common dietary oils (this is due to their impact on oil viscosity). We further characterize how these sensors may be engineered to exhibit varying sensitivities, their mechanical and absorptive properties, and, last, their potential in measuring oil content/composition directly from foods. Our primary advancement is in the increased rate of sensitivity of our sensor where in previous studies,³⁹ alongside demonstrating various methods and sensing schemes that are feasible to implement and test.

Key characteristics of these sensors include their food-safe composition, low cost and ease of synthesis, and facile **ACS Applied Bio Materials**

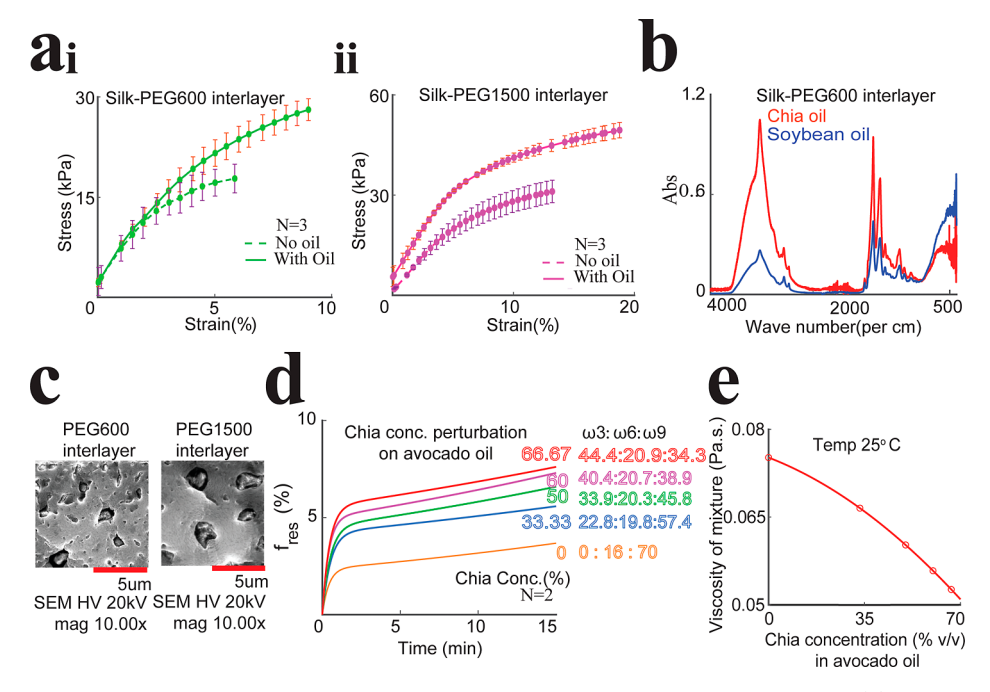


Figure 2. (a) Mechanical behavior of PEG600- and PEG1500-formed porous biopolymers, with and without oil. (b) FTIR spectroscopy analysis of the silk-PEG600 interlayer infused with chia oil (high ω 3) and soybean oil (high ω 6). (c) SEM of PEG600- and PEG1500-formed silk biopolymer. (d) Resonant frequency shift ($f_{\rm res}$) over time of our biosensor in mixtures of chia oil in an avocado oil (AO, high ω 9) possessing different omega fatty acid ratios (ω 3/ ω 6/ ω 9). (e) Viscosity of the oil mixtures at 25 °C, showing a decreasing trend in viscosity with increasing chia oil concentration.

integration with pre-existing foodware and packaging. This aligns perfectly with the emerging needs in precision nutrition, where accessible and straightforward tools for nutritional analysis are in increasing demand. Our sensors' ability to interact seamlessly with everyday food-related items underscores their potential to transform at-home nutrition measurements, offering a practical solution to monitor dietary oil and potential health implications in real-time.

2. METHODOLOGY

The broad coupled split ring resonator (BC-SRR) is composed of two conductive plates separated by a dielectric interlayer situated between them. Each plate features a single split, aligned in such a way that the splits are oriented in opposite directions, as depicted in Figure 1a. An external magnetic field, perpendicular to the plane of the plates, induces excitation in the BC-SRR, facilitating the circulation of currents. An electric field is established across the gaps due to the accumulation of charge at the splits of the plates, contributing to stored magnetic and electric fields within the resonator. These fields generate a resonant spectral response, characterizing the structure as an electromagnetic resonator. Under stable conditions, where the mechanical dimensions and the permittivity of the interlayer remain unchanged, the resonant frequency is constant over time. Through the introduction of environmentally sensitive interlayers that respond to external stimuli (such as changes in thickness or variations in permittivity), this resonator becomes a sensor. This adaptation allows for dynamic responses to environmental changes, providing a versatile wireless sensing mechanism. 36-40

The core component of the sensor proposed in this publication is an engineered porous silk fibroin biopolymer positioned between two metal electrodes in the form of a BC-SRR, presented in Figure 1a. This biopolymer acts as the

bioamplifier of the sensor—as oil/fat permanently absorbs into the membrane, as illustrated in Figure 1b, the effective capacitance of the membrane changes as high-permittivity water is replaced by this oil. This then modulates the spectral response of the resonator, reducing its resonant frequency.

Integral to this process is modification of the silk biopolymer to include open pores. This is formed via deposition of silk fibroin and PEG solution that are drop-casted onto the bottom layer of the broadside-coupled split ring resonator, as shown in Figure 1c. Polymer thickness is controlled to a thickness of 22 μ m via calculation of deposited material volume, whereas pore size can be modified via PEG molecular weight (herein studied including PEG600 and PEG1500). Upon drying, the final sensor is assembled and subjected to a heat press step at a temperature of 85 °C for 1 min. This step not only ensures the bonding of the layers but also imparts structural and chemical stability to the sensor via crystallization of the silk biopolymer that stabilizes it in aqueous environments. Following the heat press step, the sensor is placed in a desiccator overnight. The final step in the fabrication process involved immersing the sensor in deionized water (DI) for a period of 24 h to leach out the PEG polymer. The final result is a porous silk biopolymer.

Oil preferentially penetrates these porous biopolymer films due to silk fibroin's hydrophobic nature. This penetration rate is positively related to pore size and inversely related to viscosity (from the flow rate in channels). The viscosity of oils is significantly influenced by the fatty acid composition. For example, saturated fats, known for their high viscosity, offer a prime example of this. Their molecular structure is characterized by carbon atoms fully saturated with hydrogen and lacking double bonds, resulting in straight linear chains that pack closely together. This close packing increases intermolecular forces, leading to a higher viscosity. Decreasing the saturation level of fatty acids thus will reduce the viscosity

of oils, as evidenced in several studies. 45–47 In this way, dietary oil viscosity can be considered a surrogate measure of fatty acid composition as dietary oils are formed primarily of triglycerides. Despite these variations in viscosity due to fatty acid composition, dietary oils exhibit similar dielectric permittivities, largely independent of their fatty acid composition. For instance, the dielectric constants of olive, canola, soybean, and coconut oils range narrowly between 3.02 and 3.1, reflecting this similarity despite their vastly different fatty acid profiles. 48

In our sensors, oils with lower viscosities (such as omega-3-rich chia seed and salmon oils) exhibit higher flow rates and penetrate more rapidly into the biosensor. Conversely, oils with higher viscosities, like those rich in omega-9 or saturated fats, exhibit lower flow rates and infiltrate slower into the biosensor. This selective absorption leads to a permanent alteration in the biopolymer matrix's effective dielectric constant (ε') when exposed to oils or fats as these molecules replace water. The speed and efficiency of this absorption affects the sensor's capacitance measurements and is reflected in the sensor's spectral properties (or resonant frequency) where $f_{\rm res} = \frac{1}{\sqrt{({\rm LC})}}$. Sensors are then wirelessly probed via a

remote inductive link with a readout coil directly wired to a vector network analyzer (VNA). A detailed schematic diagram is shown in Supporting Information, Figure S1.

We employed finite-difference time-domain simulations using CST studio suite software to model the impact of oil absorption into biosensors. We attempted to capture elements related to sensor geometry and a porous biopolymer. Interlayer porosity is partially replicated by an array of holes in the biopolymer. These simulations yield insights into sensor performance. A detailed analysis of the electric field distribution of the sensor is shown in Supporting Information, Figures S2 and S3. The S_{11} magnitude response derived from our simulations is shown in Figure 1d. Oils, upon entering the sensor, gradually displace water molecules within the porous interlayer. This interaction causes an alteration in the effective permittivity of the biopolymer, observed as a shift in resonant frequency from higher values (where water dominates the pores $\varepsilon_r \sim 78$) to a lower one (where oil now replaces water ε_r \sim 3) as the pores are progressively replaced by oil. This highlights the inverse relationship between the sensor capacitance and oil absorption.

3. RESULTS AND DISCUSSION

3.1. Characterization of Porous Silk Biopolymer in **Oils.** We first performed comparative mechanical analysis of PEG600- and PEG1500-formed porous silk biopolymers, both with and without oil. Results are shown in [Figure 2a(i,ii)] and obtained using a dynamic mechanical analyzer. A comparison with solid silk film is shown in Supporting Information, Figure S4. Such experiments allow us to gain insights into oil penetration and how this may impact sensor behavior. For PEG600-formed sensors, introduction of oil increased the elastic modulus from 7.24 to 7.56 kPa while enhancing the ductility from 5.86 to 9.01%. This was accompanied by increases in the strength and yield stress. Comparatively, PEG1500-formed porous biopolymers without oil exhibited lower stiffness and higher ductility in comparison to PEG600formed porous biopolymers. These biopolymer films, however, saw more marked rises in stiffness, ductility, and strength when immersed for the same amount of time in oil. These larger

changes, particularly the increase in ductility and stress-bearing capacity upon oil incorporation, suggest the more responsive nature of PEG1500-formed biopolymer films. We further characterized the structures of membranes formed from different PEG molecular weights via scanning electron microscopy (SEM). Utilization of PEG1500 resulted in larger pore size openings as opposed to PEG600, suggesting at the source of variances found in the mechanical and absorptive properties of the two formed films (Figure 2c). PEG600formed biopolymer exhibited more heterogeneous porosity. In contrast, the PEG1500-formed biopolymer exhibits a larger pore size and a more homogeneous pore distribution. The pores exhibit uniformity in shape and refined edge definition, leading to a comparatively smoother surface topography. As pore size directly relates to the flow rate in channels, this is presumed to be the source of the higher absorption and larger mechanical shifts of these films when immersed in oil. The mechanical performance of these porous films can be further compared to solid silk fibroin (without PEG) shown in Supporting Information, Figure S4.

We next sought to study different oils exhibiting differential viscosities and fatty acid contents and test how they interact with our biopolymer. We first characterized the FTIR absorption spectral comparison of PEG600-formed biopolymer films shown in Figure 2b immersed in chia (high in ω 3) and soybean oils (high in ω 6). Within the chia oil-infused film's spectrum, noticeable peaks in the 3000-2800 cm⁻¹ range are prominently visible, signifying the oil's rich omega-3 fatty acid content that has penetrated the biopolymer. These peaks are distinguished by their characteristic C-H stretching vibrations. Conversely, the spectrum of the soybean oil-infused film also features peaks in this zone, yet they exhibit a subtly altered pattern, reflecting its comparatively higher omega-6 fatty acid concentration. The key difference, however, is in the intensity of peaks as chia oil clearly absorbs the porous biopolymer at a higher rate than soybean. The transmittance of these films is further detailed in Supporting Information, Figure S5, indicating differences in the absorbed volume of oil in the biopolymer.

We next sought to calibrate our passive wireless biosensor response to dietary oils of differing viscosity. These sensors need only to be exposed on its surface to oil and with minimal volume required to fill the sensor itself (oil tends to coat surfaces). While we have previously utilized down to 100 μ L on top of our sensors, theoretically the amount needed is much lower as the oil simply must be enough to fill the membrane of the sensor. This open sensor membrane volume depends on sensor dimensions but can be estimated as below 1 μ L. This minimal absorption ensures that the original content of the oil remains largely unaffected for practical purposes. The integrity of the bulk oil sample is maintained, making the testing process nondestructive. We created dietary oils of controlled viscosity by mixing high-viscosity avocado oil (high ω 9) with lowerviscosity chia oil (high ω 3), whose measured viscosity is shown in Figure 2e. These dietary oil mixtures exhibit reducing viscosity as related to the proportion of chia in avocado (quantified here as %). The responses of our sensors to these varying mixtures are demonstrated in (Figure 2d). In response to oil, our sensors exhibit a large initial dynamic sensor response (in this case, the rate of resonant frequency shift), before this response tapers. This is indicative of how dietary oil appears to penetrate the porous biopolymer films over time, whose penetration rate reduces as pores become filled and the

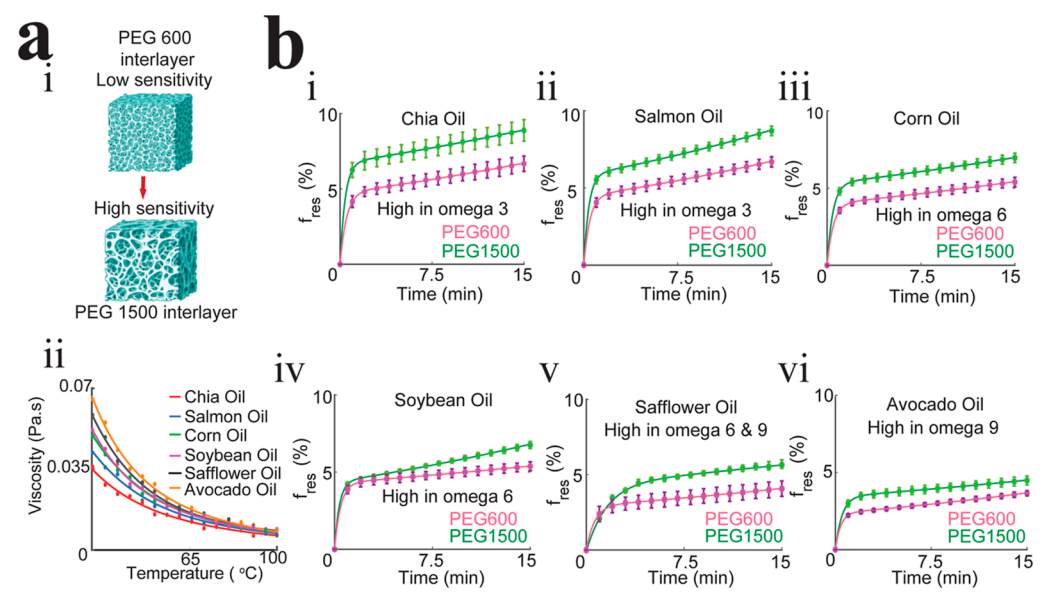


Figure 3. (a) (i) Schematic representations of PEG 600- and PEG 1500-formed porous biopolymer interlayers. (ii) Viscosities of our various tested dietary oils vs temperature. Omega fatty acid composition is given in percentages here (w3,w6,w9). Chia (60,20,11) and salmon (36,4,40) oils are high in omega-3 fatty acids. Corn (1,53,27) and soybean (7,50,23) oils are high in omega-6 fatty acids. Safflower oil (0,13,75) is high in omega-9 fatty acids, as is avocado oil (0,16,70) oil. The slightly higher viscosity of avocado oil is potentially attributable to its higher saturated fat content. (b) Graphical data from (i–vi) showing the resonant frequency shift (f_{res}) as a percentage over time for different oils absorbed by PEG 600- and PEG 1500-formed porous biopolymer RF biosensors. The graphs are divided into categories based on the type of oil and its predominant omega fatty acid. N = 2.

biopolymer inches closer to its carrying capacity for oil. Either the dynamic or total response at a fixed time (i.e., 10 min) can be correlated with local oil presence and fatty acid approximation. However, due to sensor nonlinearity, it must be continuously measured to obtain accurate results. Initially, the viscosity (as in Figure 2e) is at its highest with pure avocado oil at 0.075 Pa·s. As chia oil is introduced with various concentrations, we observe a decrease in viscosity of the oil mixture, with a drop to 0.052 Pa s at the highest chia concentration of 66.67%.

Our biosensors exhibit an increasing response with increasing proportions of chia oil, exhibiting larger increases in both the initial rate and total percentage shift in sensor resonant frequencies. The calibration curves likely reflect a point of saturation where further increases in chia concentration result in a smaller relative change in the frequency shift, suggesting that the sensor's response to viscosity may approach a plateau. Note that the omega fatty acid composition of these mixtures is additionally shown in Figure 2d.

3.2. Differential Sensing of Oil and Fatty Acid Composition with Porous Biopolymer RF Sensors. We next characterized the biosensor response to common dietary oils consumed in the typical diet. This is encompassed by a set including oils of neutral health properties (avocado and safflower oils, high in $\omega 9$), potentially negative health properties (soybean and corn oils, high in ω 6), and positive health properties (salmon and chia oils, high in ω 3). We characterized the viscosity of these oils in Figure 3a(ii). Our measured viscosities matched results from existing publications as we found that dietary oils exhibited viscosities related to fatty acid composition, where oils dominated by $\omega 3$, $\omega 6$, and ω 9 possessed increasing viscosity in that order. Our RF sensor response curves are presented in (Figure 3b) demonstrating distinct sensitivity of our porous biopolymer RF biosensor to these different oils. Healthy chia and salmon oils, which are

high in polyunsaturated omega-3 fatty acids, exhibit steeper resonant frequency shift curves Figure 3b(i,ii). The marginally steeper curve for chia oil, as compared to salmon oil, underscores the sensitivity of the sensor to even subtle differences in viscosity (salmon oil possesses higher percentages of saturated fat that lead to slightly higher viscosity).

When oils higher in omega-6 fatty acids, such as corn and soybean oils, Figure 3b(iii,iv), are introduced to the sensor, the frequency shifts are less pronounced. These oils, rich in polyunsaturated but with a different composition of fatty acids compared to omega-3 oils, have higher viscosities, which could be attributed to the varying ratios of polyunsaturated to monounsaturated fats. Safflower oil, containing some omega-6 and significant amounts of omega-9 fatty acids, presents a unique profile Figure 3b(v). While still rich in polyunsaturated fats, the presence of omega 9, which are monounsaturated, could be affecting its interaction with the sensor material, as monounsaturated fats tend to be more viscous and can form more ordered structures than polyunsaturated fats. Avocado oil, an emerging healthy alternative to omega-6-dominated seed oils, is predominantly composed of monounsaturated omega-9 fats. These possess our highest studied viscosity and lead to the least-dynamic and total sensor response Figure

When compared to the PEG600-formed porous biopolymer, PEG1500-formed sensors exhibited greater dynamic sensitivity when exposed to the same oil, again indicating the increased sensitivity imparted by larger pore size. These response curves serve as an illustration of the unique sensing capabilities of these sensors, which are both readily engineerable and exhibit unique sensitivity to both oil presence and its fatty acid composition (or healthiness). In practice, we expect that smaller PEG molecular weight could reduce sensitivity, while higher PEG molecular weight could compromise the reliability

and durability of the sensor. Such factors need to be weighed against their application.

Our insights pave the way into utilizing such sensors in athome health monitoring and nutritional tracking applications, where the characterization of oil consumption and properties can yield key precision information to users; for example, our sensors can act for broad characterization of the nutritive quality of measured dietary oil through assessment of whether it is omega 3-, omega 6-, or omega 9-dominated. This fundamental assessment can assist users in understanding whether they are missing specific elements from their diet (such as omega 3s) or consuming too much unhealthy seed oil (omega 6s). The sensor on its own does not measure the total consumption, however. We anticipate it may be possible to array this sensor with volumetric measures for precision measurement of both oil nutritive quality and its total consumption. Table S1 presents the distinct dynamic response of the sensors when exposed to various edible oils. This data can be used to categorize oil type while monitoring in real time.

3.3. Practical Implementations of Oil-Monitoring RF Biosensors. Oils are used in diverse culinary preparations. With our RF sensors, it is possible to track and monitor oils resulting from different culinary practices. Here, we explore the responsiveness of this sensor when subjected to oils used in potato cooking shown in Figure 4a,b and salad mixing shown

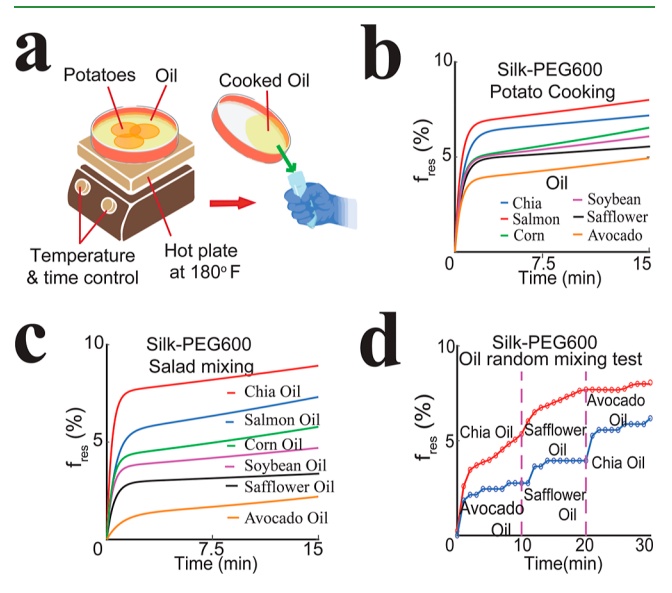


Figure 4. (a) Diagram of the potential use case for our sensors in measuring oils used during food preparation or cooking at 180 °F. (b) Resonance frequency shift over time of different oils used for potato cooking after having cooled to room temperature. (c) RF sensor response to different oils used as dressing for a salad. (d) Sensor response to sequential presentation of different oils. Dynamic response to different oils depends on the previous exposure (fill of the biopolymer) of the sensor.

in Figure 4c. This analysis underscores not only the sensor's potential in real-time monitoring of oil presence from actual foods but also its application in potentially understanding or assessing the healthiness of oils from these prepared foods. We first assessed the response of our sensor to liquids extracted after cooking potatoes in a variety of oils (the same set as used in Figure 3). As expected, chia and salmon oils, both high in omega-3 fatty acids, show (in Figure 4b) the highest dynamic

sensor response and the highest resonant frequency shifts when measured at 10 min.

Corn and soybean oils (richer in w6) and safflower oils (richer in w6,9) exhibit comparatively lower dynamic sensor response. Avocado oil, high in omega 9, shows the least change. Here, trends in sensor sensitivity to oils match results expected from our benchtop studies.

These results can be contrasted against measurements from liquids extracted after salads were mixed with different oil dressings. The $f_{\rm res}$, shifts here both follow trends related to oil fatty acid composition but also better match benchtop studies from earlier. Chia oil, with its lower viscosity, elicits the strongest sensor response.

The trend from chia to avocado oil follows a descending order, with avocado oil again showing the lowest shift. This consistent trend with both cooking and mixing suggests that the sensor is effectively detecting aspects of fatty acid composition and potentially healthiness of the oil. In further contrasting cooked vs mixed oil responses, we find that after cooking, more viscous oils exhibited slightly higher dynamic and total sensor response than expected from benchtop studies. We attribute this to either chemical transformation generated during the cooking process (that appear to impact more strongly the viscosity of more viscous oils) or residual heat from the cooking process itself. This may mean that some knowledge of the cooking process (or temperature) may be necessary for the more accurate classification of cooked oils. A graph comparing sensor response before and after cooking has been added to Supporting Information, Figure S6.

We last sought to preliminarily study how our sensors may potentially be used to dynamically characterize oils of different compositions (or viscosity). This may give sensors lifetime beyond single-use measurement (where dynamic sensor response can characterize oil) or continuous measurement of oil exposure over a limited lifetime (through tracking penetration of oil from the environment until the biopolymer is filled). Figure 4d illustrates the percentage resonant frequency shift over time of our RF oil sensor exposed to a sequence of oils with varying fatty acid compositions. The blue curve begins with avocado oil before progressing to safflower and chia oils. This initial response to avocado oil shows a gradual increase in the fres shift, reflecting the slower absorption due to its higher viscosity. As the sequence progresses at 10 min, safflower oil is added. This leads to a jump in the dynamic and total sensor response. Finally, chia oil (added at 20 min marked dashed line) is introduced. The sensor's frequency shift escalates rapidly again with chia oil, suggesting that its lower viscosity can remain tracked in some form through sensor response if the sensor has not been significantly filled in its previous lifetime exposure to oils. In contrast, the red curve initiates with chia oil, leading to a sharp and immediate increase in fres shift, indicating rapid permeation into the biopolymer. Subsequent exposures to safflower oil and avocado oil do not heavily modulate the sensor response, indicating that previous heavy absorption of chia oil is impeding penetration of other oils into the biopolymer. These results indicate that dynamic monitoring of advanced oil properties may be possible but will need to adjust to the dynamic carrying capacity of the sensor (that likely relates to the resonant frequency shift). The sensor on its own remains feasible (as we have tested on oils that people consume) and can be useful for testing bottled oils or foods known to be dressed or cooked in pure oil. Everyone uses

bottled oils, and many foods are dressed/cooked in oil, and this on its own has utility. One potential use-case may be "fake" oils, where cheaper soybean or corn oil replaces or adulterates more expensive chia or avocado oils. Given fake oil, one may utilize our technique to rapidly assess if the oil behaves as expected. The porous silk fibroin biopolymer used in our sensor selectively absorbs oils from environmental liquids due to its hydrophobic nature. On its own, the sensor appears to be suitable for measuring pure bottled oils or oil-dominated food liquids (such as from fried foods). However, their accuracy may reduce oils that may have been mixed with other nonoil ingredients (such as water) in postfood preparation scenarios—this may modulate the rate of oil penetration into the biopolymer. We anticipate that our sensor may be utilized alongside other sensors that directly monitor the permittivity of the test oil. These could potentially distinguish water and solid contents that have been mixed in with the oil under test. Such sensors could readily be made using electrodes that directly probe the oil itself.

4. CONCLUSIONS

Here, we study low-cost, accessible, and biocompatible RF biosensors for oil and fatty acid content monitoring. The unique features of these sensors make them ideal for many emerging applications in precision nutrition and home health monitoring. The sensor's compact size, wireless readout, and flexibility make them ideal in interfacing with existing food ware or food packaging. Furthermore, they are composed exclusively of food-safe components (metal foils and biopolymer), making them viable for utilization directly on consumed foods. Silk fibroin, derived from the cocoons of silkworms, is a well-studied biopolymer known for its excellent biocompatibility. It has been widely used in biomedical applications such as sutures, wound dressings, and drug delivery systems, demonstrating its safety for direct contact with biological tissues and cells. Silk fibroin is also considered safe for food applications. Aluminum foil is commonly used in food packaging and cooking and is approved by food safety regulatory agencies for direct contact with food. Silk biopolymer, however, is biodegradable and could potentially break down over time in specific enzymatic environments. Bulk erosion, which affects the entire material uniformly, can reduce the overall density and structural integrity of the silk fibroin biopolymer, thereby altering its dielectric properties and affecting the sensor capacitance and resonant frequency. This would additionally modulate the sensitivity of the sensor. Surface erosion, as noted by the reviewer, could cause gaps between the metal and biopolymer, potentially destabilizing the structure and facilitating the breakdown of the sensor itself. To mitigate these effects, silk biopolymer is crystallized via water annealing process, enhancing the biopolymer's resistance to degradation⁴⁹ and enhancing its shelf life.

In contrast to existing oil-monitoring chemical analysis techniques, they require no sample preparation or specialized equipment/procedures. These RF biosensors can be measured using modern VNA tools that are wearable and compact/deployable. VNAs are highly precise instruments capable of characterizing the sensor's electromagnetic properties by measuring the reflection coefficient (S_{11} parameter). For home use, commercially available portable Nano-VNA and Mini-VNA are suitable as these come in small sizes and low-cost. The output power from our VNA is 100 mW, which is converted into a magnetic field to probe our sensor. Notably,

this power is significantly less than NFC protocols that can deliver up to 1 W in RF magnetic power and are rated safe near people. In contrast to our proposed measurement approach, commercial rheometers are relatively more expensive, are immobile (carried around in a heavy case), and are significantly larger (composed of multiple metal bars to be assembled). The lowest cost and more compact RF readers can be deployed or utilized to measure our wireless RF sensor networks that may be fused on bottles, plates, dishes, etc. Last, our sensor can be used directly from foods—this is because the sensor absorbs minimal oil volume to work. This is unlike the case for rheometers that require large volumes of liquid to perform their measurement.

We perform studies exploring the optimization, performance, and practical utilization of such sensors in monitoring dietary oil and its composition. These sensors are sensitive to oil viscosity and oil omega fatty acid composition and have potential use cases in monitoring foods cooked or prepared in oil. Our sensors' ability to interact seamlessly with everyday food-related items underscores their potential to transform athome nutrition measurements, offering a practical solution to monitor dietary oil and potential health implications in real-time.

5. EXPERIMENTAL SECTION

Details on the experimental protocols are given in the Supporting Information.

ASSOCIATED CONTENT

Supporting Information

The Supporting Information is available free of charge at https://pubs.acs.org/doi/10.1021/acsabm.4c00601.

Chemical materials, experimental protocols, schematic diagrams of experimental setup, *E* field distribution of the sensor and discussion, experimental graphs of stress vs strain of silk, FTIR spectra of the oil-absorbed interlayer film, oil viscosity graph vs temperature, 6 h long sensor response, and dynamic responses of the sensor when exposed to stimuli/oils (PDF)

AUTHOR INFORMATION

Corresponding Author

Peter Tseng — Department of Electrical Engineering and Computer Science, University of California Irvine, Irvine, California 92697, United States; Department of Biomedical Engineering, University of California Irvine, Irvine, California 92697, United States; ◎ orcid.org/0000-0001-6598-1661; Email: tsengpc@uci.edu

Authors

Kazi Khurshidi Haque Dia – Department of Electrical Engineering and Computer Science, University of California Irvine, Irvine, California 92697, United States

Alberto Ranier Escobar — Department of Biomedical Engineering, University of California Irvine, Irvine, California 92697, United States; orcid.org/0000-0002-0381-1699

Huiting Qin – Material and Manufacturing Technology Program, University of California, Irvine, California 92617, United States

Fan Ye – Department of Electrical Engineering and Computer Science, University of California Irvine, Irvine, California 92697, United States

- Abel Jimenez Department of Electrical Engineering and Computer Science, University of California Irvine, Irvine, California 92697, United States
- Md Abeed Hasan Department of Electrical Engineering and Computer Science, University of California Irvine, Irvine, California 92697, United States
- Amirhossein Hajiaghajani Department of Electrical Engineering and Computer Science, University of California Irvine, Irvine, California 92697, United States
- Manik Dautta Department of Electrical Engineering and Computer Science, University of California Irvine, Irvine, California 92697, United States
- Lei Li Department of Electrical Engineering and Computer Science, University of California Irvine, Irvine, California 92697, United States

Complete contact information is available at: https://pubs.acs.org/10.1021/acsabm.4c00601

Author Contributions

K.K.H.D. and P.T. conceptualized the project. K.K.H. D. performed the experiments with assistance from A.E., H.Q., A.J., M.A.H., A.H., and L.L. The simulations were done by F.Y. Initial studies were discussed with M.D. All the authors discussed the results. K.K.H.D. and P.T. wrote the article.

Notes

The authors declare no competing financial interest.

ACKNOWLEDGMENTS

The authors acknowledge funding from the National Science Foundation (NSF) Career Award (Award number 1942364) for supporting this work. Authors also acknowledge BioRender (online figure creating tool) as some of the components of the figures are "Created with BioRender.com". Authors also acknowledge Fishman lab of University of California Irvine for allowing authors to perform FTIR analysis.

ABBREVIATIONS

BC-SRR, broad-coupled split ring resonator; FTIR, Fourier transform infrared; GC-FID, gas chromatography flame-ionization detection; ICP-MS, inductively coupled plasmamass spectrometry; SEM, scanning electron microscopy

REFERENCES

- (1) Wu, J. H. Y.; Micha, R.; Mozaffarian, D. Dietary Fats and Cardiometabolic Disease: Mechanisms and Effects on Risk Factors and Outcomes. *Nat. Rev. Cardiol.* **2019**, *16* (10), 581–601.
- (2) Sun, L.; Zong, G.; Li, H.; Lin, X. Fatty Acids and Cardiometabolic Health: A Review of Studies in Chinese Populations. *Eur. J. Clin. Nutr.* **2021**, 75 (2), 253–266.
- (3) Hasenhuettl, G. L. Fats and Fatty Oils. In Kirk-Othmer Encyclopedia of Chemical Technology; Wiley, 2005.
- (4) Thomas, A.; Matthäus, B.; Fiebig, H.-J. Fats and Fatty Oils. In *Ullmann's Encyclopedia of Industrial Chemistry*; Wiley-VCH Verlag GmbH & Co. KGaA: Weinheim, Germany, 2015; pp 1–84.
- (5) Yang, W.-S.; Chen, Y.-Y.; Chen, P.-C.; Hsu, H.-C.; Su, T.-C.; Lin, H.-J.; Chen, M.-F.; Lee, Y.-T.; Chien, K.-L. Association between Plasma N-6 Polyunsaturated Fatty Acids Levels and the Risk of Cardiovascular Disease in a Community-Based Cohort Study. *Sci. Rep.* **2019**, *9* (1), 19298.
- (6) Wang, Y.; Fang, Y.; Witting, P. K.; Charchar, F. J.; Sobey, C. G.; Drummond, G. R.; Golledge, J. Dietary Fatty Acids and Mortality Risk from Heart Disease in US Adults: An Analysis Based on NHANES. Sci. Rep. 2023, 13 (1), 1614.

- (7) Endo, Y. Analytical Methods to Evaluate the Quality of Edible Fats and Oils: The JOCS Standard Methods for Analysis of Fats, Oils and Related Materials (2013) and Advanced Methods. *J. Oleo Sci.* **2018**, *67* (1), 1–10.
- (8) Ratnayake, W. M. N.; Galli, C. Fat and Fatty Acid Terminology, Methods of Analysis and Fat Digestion and Metabolism: A Background Review Paper. *Ann. Nutr. Metab.* **2009**, *55* (1–3), 8–43. (9) Kunau, W.-H. Synthesis of Unsaturated Fatty Acids. *Chem. Phys.*
- Lipids 1973, 11 (4), 254–269.
- (10) James, A. T. Determination of the Degree of Unsaturation of Long Chain Fatty Acids by Gas-Liquid Chromatography. *J. Chromatogr. A* **1959**, *2*, 552–561.
- (11) Gurr, M. I. The Biosynthesis of Unsaturated Fatty Acids. In *Biochemistry of Lipids*; Elsevier, 1974; pp 181–235.
- (12) Djuricic, I.; Calder, P. C. Beneficial Outcomes of Omega-6 and Omega-3 Polyunsaturated Fatty Acids on Human Health: An Update for 2021. *Nutrients* **2021**, *13* (7), 2421.
- (13) Jiang, H.; Wang, L.; Wang, D.; Yan, N.; Li, C.; Wu, M.; Wang, F.; Mi, B.; Chen, F.; Jia, W.; Liu, X.; Lv, J.; Liu, Y.; Lin, J.; Ma, L. Omega-3 Polyunsaturated Fatty Acid Biomarkers and Risk of Type 2 Diabetes, Cardiovascular Disease, Cancer, and Mortality. *Clin. Nutr.* **2022**, *41* (8), 1798–1807.
- (14) Saini, R. K.; Keum, Y.-S. Omega-3 and Omega-6 Polyunsaturated Fatty Acids: Dietary Sources, Metabolism, and Significance A Review. *Life Sci.* **2018**, *203*, 255–267.
- (15) Erkkilä, A.; de Mello, V. D. F.; Risérus, U.; Laaksonen, D. E. Dietary Fatty Acids and Cardiovascular Disease: An Epidemiological Approach. *Prog. Lipid Res.* **2008**, 47 (3), 172–187.
- (16) Foley, M.; Ball, M.; Chisholm, A.; Duncan, A.; Spears, G.; Mann, J. Should Mono- or Poly-Unsaturated Fats Replace Saturated Fat in the Diet? *Eur. J. Clin. Nutr.* **1992**, *46* (6), 429–436.
- (17) Hodson, L.; Skeaff, C.; Chisholm, W.-A. The Effect of Replacing Dietary Saturated Fat with Polyunsaturated or Monounsaturated Fat on Plasma Lipids in Free-Living Young Adults. *Eur. J. Clin. Nutr.* **2001**, *55* (10), 908–915.
- (18) Welty, F. K. Omega-3 Fatty Acids and Cognitive Function. Curr. Opin. Lipidol. 2023, 34 (1), 12–21.
- (19) Kerdiles, O.; Layé, S.; Calon, F. Omega-3 Polyunsaturated Fatty Acids and Brain Health: Preclinical Evidence for the Prevention of Neurodegenerative Diseases. *Trends Food Sci. Technol.* **2017**, *69*, 203–213.
- (20) Farag, M. A.; Gad, M. Z. Omega-9 Fatty Acids: Potential Roles in Inflammation and Cancer Management. *J. Genet. Eng. Biotechnol.* **2022**, 20 (1), 48.
- (21) Sherazi, S. T. H.; Kandhro, A.; Mahesar, S. A.; Bhanger, M. I.; Talpur, M. Y.; Arain, S. Application of Transmission FT-IR Spectroscopy for the Trans Fat Determination in the Industrially Processed Edible Oils. *Food Chem.* **2009**, *114* (1), 323–327.
- (22) Cañada, M. J. A.; Medina, A. R.; Lendl, B. Determination of Free Fatty Acids in Edible Oils by Continuous-Flow Analysis with FT-IR Spectroscopic Detection. *Appl. Spectrosc.* **2001**, *55* (3), 356–360.
- (23) Ismail, A. A.; van de Voort, F. R.; Emo, G.; Sedman, J. Rapid Quantitative Determination of Free Fatty Acids in Fats and Oils by Fourier Transform Infrared Spectroscopy. *J. Am. Oil Chem. Soc.* **1993**, 70 (4), 335–341.
- (24) Al-Alawi, A.; van de Voort, F. R.; Sedman, J. New FTIR Method for the Determination of FFA in Oils. *J. Am. Oil Chem. Soc.* **2004**, *81* (5), 441–446.
- (25) Azizian, H.; Kramer, J. K. G. A Rapid Method for the Quantification of Fatty Acids in Fats and Oils with Emphasis on Trans Fatty Acids Using Fourier Transform near Infrared Spectroscopy (FT-NIR). *Lipids* **2005**, *40* (8), 855–867.
- (26) Sherazi, S. T. H.; Talpur, M. Y.; Mahesar, S. A.; Kandhro, A. A.; Arain, S. Main Fatty Acid Classes in Vegetable Oils by SB-ATR-Fourier Transform Infrared (FTIR) Spectroscopy. *Talanta* **2009**, *80* (2), 600–606.
- (27) Siang, G. H.; Makahleh, A.; Saad, B.; Lim, B. P. Hollow Fiber Liquid-Phase Microextraction Coupled with Gas Chromatography-

- Flame Ionization Detection for the Profiling of Fatty Acids in Vegetable Oils. *J. Chromatogr. A* **2010**, 1217 (52), 8073–8078.
- (28) Jalali-Heravi, M.; Vosough, M. Characterization and Determination of Fatty Acids in Fish Oil Using Gas Chromatography-Mass Spectrometry Coupled with Chemometric Resolution Techniques. *J. Chromatogr. A* **2004**, *1024* (1–2), 165–176.
- (29) Jamieson, G. R.; Reid, E. H. The Analysis of Oils and Fats by Gas Chromatography. *J. Chromatogr. A* **1965**, *17*, 230–237.
- (30) Fabbri, D.; Baravelli, V.; Chiavari, G.; Prati, S. Profiling Fatty Acids in Vegetable Oils by Reactive Pyrolysis-Gas Chromatography with Dimethyl Carbonate and Titanium Silicate. *J. Chromatogr. A* **2005**, *1100* (2), 218–222.
- (31) Qu, S.; Du, Z.; Zhang, Y. Direct Detection of Free Fatty Acids in Edible Oils Using Supercritical Fluid Chromatography Coupled with Mass Spectrometry. *Food Chem.* **2015**, *170*, 463–469.
- (32) Liu, M.; Wei, F.; Lv, X.; Dong, X.; Chen, H. Rapid and Sensitive Detection of Free Fatty Acids in Edible Oils Based on Chemical Derivatization Coupled with Electrospray Ionization Tandem Mass Spectrometry. *Food Chem.* **2018**, *242*, 338–344.
- (33) Bi, X.; Jin, Y.; Li, S.; Gao, D.; Jiang, Y.; Liu, H. Rapid and Sensitive Determination of Fatty Acids in Edible Oil by Liquid Chromatography-Electrospray Ionization Tandem Mass Spectrometry. Sci. China Chem. 2014, 57 (3), 447–452.
- (34) Thurnhofer, S.; Vetter, W. A Gas Chromatography/Electron Ionization-Mass Spectrometry-Selected Ion Monitoring Method for Determining the Fatty Acid Pattern in Food after Formation of Fatty Acid Methyl Esters. J. Agric. Food Chem. 2005, 53 (23), 8896–8903.
- (35) Zehethofer, N.; Pinto, D. M.; Volmer, D. A. Plasma Free Fatty Acid Profiling in a Fish Oil Human Intervention Study Using Ultraperformance Liquid Chromatography/Electrospray Ionization Tandem Mass Spectrometry. *Rapid Commun. Mass Spectrom.* **2008**, 22 (13), 2125–2133.
- (36) Dia, K. K. H.; Hajiaghajani, A.; Escobar, A. R.; Dautta, M.; Tseng, P. Broadside-Coupled Split Ring Resonators as a Model Construct for Passive Wireless Sensing. *Adv. Sens. Res.* **2023**, 2 (10), 2300006.
- (37) Dautta, M.; Alshetaiwi, M.; Escobar, A.; Torres, F.; Bernardo, N.; Tseng, P. Multi-Functional Hydrogel-Interlayer RF/NFC Resonators as a Versatile Platform for Passive and Wireless Biosensing. *Adv. Electron. Mater.* **2020**, *6* (4), 1901311.
- (38) Dautta, M.; Alshetaiwi, M.; Escobar, J.; Tseng, P. Passive and Wireless, Implantable Glucose Sensing with Phenylboronic Acid Hydrogel-Interlayer RF Resonators. *Biosens. Bioelectron.* **2020**, *151*, 112004.
- (39) Dautta, M.; Dia, K. K. H.; Hajiaghajani, A.; Escobar, A. R.; Alshetaiwi, M.; Tseng, P. Multiscale, Nano- to Mesostructural Engineering of Silk Biopolymer-Interlayer Biosensors for Continuous Comonitoring of Nutrients in Food. *Adv. Mater. Technol.* **2022**, *7* (2), 2100666.
- (40) Tseng, P.; Napier, B.; Garbarini, L.; Kaplan, D. L.; Omenetto, F. G. Functional, RF-Trilayer Sensors for Tooth-Mounted, Wireless Monitoring of the Oral Cavity and Food Consumption. *Adv. Mater.* **2018**, *30* (18), 1703257.
- (41) Hajiaghajani, A.; Afandizadeh Zargari, A. H.; Dautta, M.; Jimenez, A.; Kurdahi, F.; Tseng, P. Textile-Integrated Metamaterials for near-Field Multibody Area Networks. *Nat. Electron.* **2021**, *4* (11), 808–817
- (42) Hajiaghajani, A.; Rwei, P.; Afandizadeh Zargari, A. H.; Escobar, A. R.; Kurdahi, F.; Khine, M.; Tseng, P. Amphibious Epidermal Area Networks for Uninterrupted Wireless Data and Power Transfer. *Nat. Commun.* **2023**, *14* (1), 7522.
- (43) Dautta, M.; Hajiaghajani, A.; Ye, F.; Escobar, A. R.; Jimenez, A.; Dia, K. K. H.; Tseng, P. Programmable Multiwavelength Radio Frequency Spectrometry of Chemophysical Environments through an Adaptable Network of Flexible and Environmentally Responsive, Passive Wireless Elements. *Small Sci.* **2022**, *2* (6), 2200013.
- (44) Fountain, J. N.; Hawker, M. J.; Hartle, L.; Wu, J.; Montanari, V.; Sahoo, J. K.; Davis, L. M.; Kaplan, D. L.; Kumar, K. Towards Non-

- stick Silk: Tuning the Hydrophobicity of Silk Fibroin Protein. ChemBioChem 2022, 23 (22), No. e202200429.
- (45) Yalcin, H.; Toker, O. S.; Dogan, M. Effect of Oil Type and Fatty Acid Composition on Dynamic and Steady Shear Rheology of Vegetable Oils. *J. Oleo Sci.* **2012**, *61* (4), 181–187.
- (46) Santos, J. C. O.; Santos, I. M. G.; Souza, A. G. Effect of Heating and Cooling on Rheological Parameters of Edible Vegetable Oils. *J. Food Eng.* **2005**, *67* (4), 401–405.
- (47) Kim, J.; Kim, D. N.; Lee, S. H.; Yoo, S.-H.; Lee, S. Correlation of Fatty Acid Composition of Vegetable Oils with Rheological Behaviour and Oil Uptake. *Food Chem.* **2010**, *118* (2), 398–402.
- (48) Peñaloza-Delgado, R.; Olvera-Cervantes, J. L.; Sosa-Morales, M. E.; Kataria, T. K.; Corona-Chávez, A. Dielectric Characterization of Vegetable Oils during a Heating Cycle. *J. Food Sci. Technol.* **2021**, 58 (4), 1480–1487.
- (49) Zhao, M.; Qi, Z.; Tao, X.; Newkirk, C.; Hu, X.; Lu, S. Chemical, Thermal, Time, and Enzymatic Stability of Silk Materials with Silk I Structure. *Int. J. Mol. Sci.* **2021**, 22 (8), 4136.